e-Journal of Nondestructive Testing - ISSN 1435-4934 - www.ndt.net

EWSHM 2024
11th European Workshop on Structural Health Monitoring

Early detection of structural damage in UHPFRC structures through the combination of acoustic emission and ultrasonic stress wave monitoring

Numa BERTOLA [1,2], Thomas SCHUMACHER [1,3], Ernst NIEDERLEITHINGER [4], Eugen BRÜHWILER[1]

[1] Ecole Polytechnique Fédérale de Lausanne (EPFL), Structural Engineering Institute, Lausanne, Switzerland, eugen.bruehwiler@epfl.ch

[2] University of Luxembourg, Department of Engineering, Esch-sur-Alzette, Luxembourg, numa.bertola@uni.lu

[3] Portland State University, Civil and Environmental Engineering, Portland, USA, thomas.schumacher@pdx.edu

[4] Bundesanstalt für Materialforschung und -prüfung, Berlin, Germany, ernst.niederleithinger@bam.de

Abstract. Ultra-High-Performance Fiber-Reinforced Cementitious Composite (UHPFRC) offers several advantages compared to concrete, notably due to the strain hardening behavior under tensile actions. Structures made of this composite material are lightweight and highly durable, thanks to the UHPFRC waterproofing quality. Nonetheless, the tensile behavior leads to a different cracking pattern than conventional concrete and is not fully understood yet. This paper presents a combined approach using both passive ultrasonic (US) stress wave (or acoustic emission) and active US stress wave monitoring to localize and quantify damage progression in a full-scale UHPFRC beam during experimental load testing. The proposed monitoring approach involves 24 US transducers that are embedded randomly throughout a 4.2-meter-long laboratory UHPFRC T-beam. Continuous monitoring enabled accurate localization of US stress sources caused by loading-induced cracking as well as from pulses generated by the embedded US transducers. This study shows that it is possible to predict the location and shape of the macro-crack that is linked to structural failure early on, i.e., just after the end of the elastic domain. This combined approach opens new possibilities to monitor the structural behavior and detect damage on UHPFRC structures before they affect the structural behavior in terms of deflection and strain.

Keywords: Structural health monitoring; Acoustic emission monitoring; Ultrasonic stress wave monitoring; Ultra-High-Performance Fibre Reinforced Cementitious Composite; Embedded ultrasonic transducers; Experimental laboratory testing; Crack monitoring.

https://doi.org/10.58286/29698

1. Introduction

Structural health monitoring (SHM) is useful both for monitoring of existing structures as well as for evaluating the performance of structural systems made with new materials.

Ultra-High-Performance Fibre-Reinforced Cementitious Composite (UHPFRC) offers new perspectives as this cementitious material has highest mechanical properties and durability compared to all other materials bound with cement [1,2]. UHPFRC is made of a highly compact paste with a high cement content (700 to 1000 kg/m^3) with a low water/binder ratio (equal to 0.13–0.17), fine-hard particles with a maximum grain size of 1 mm, additives, superplasticizer, and 3-vol % of short slender steel fibers [3]. Over the past two decades, this material has been employed in hundreds of bridge engineering applications for both new designs and structural rehabilitation [4,5].

The mechanical properties of UHPFRC are summarized by Brühwiler [6]. Maximum characteristic values of the tensile and compressive strengths are up to 16 and 180 MPa, respectively. The elastic modulus is between 45 and 50 GPa. As the material exhibits strain-hardening behavior in tension up to deformation of 1-2‰, it means that the material remains crack-free under service conditions. UHPFRC structural elements thus have a very long durability. The tensile strength is typically further improved by adding reinforcement bars, similarly to reinforced concrete structures. The Swiss Technical Leaflet on UHPFRC (SIA 2052) was released in 2016 and updated in 2024 for the design of UHPFRC structures [7].
The development of UHPFRC's unique properties and damage evolution are of particular interest. Many studies have been made on laboratory experiments, but they usually involve destructive testing [8]. Thus, these approaches cannot be adapted for monitoring new structural elements made of UHPFRC.

This study introduces a novel non-destructive monitoring approach to monitor the evolution of UHPFRC properties at early age. The system is composed of ultrasonic (US) transducers [Model ACS S0807 [9]] that are capable of recording acoustic emissions (AE) or passive US stress waves, as well as emitting consistent pulses to produce consistent active US stress waves [10]. In this research, a 24-transducer network was embedded in a 4.2-meter laboratory T-beam made of UHPFRC prior to casting of the specimen.

This paper summarizes results from the early-age monitoring phase of the beam specimen (Phase 1) but focuses on Phase 2, during which the specimen was loaded in four-point bending to failure. In Phase 3, the specimen was placed outside the laboratory and exposed to varying environmental conditions. Analysis of Phase 3 is subject to future research.

2. Test specimen and instrumentation

A T-shaped beam made of UHPFRC using conventional Swiss-market mix, with dimensions of 4200 mm in length and 400 mm in depth was fabricated in the laboratory facility at EPFL **Fig. 1**B, C. **Fig. 1**A, C show the experimental test setup for Phase 2.

The instrumentation of Phase 1 consists of 24 US transducers and 15 thermocouples embedded within the web of the beam (**Fig. 1**C). Phase 2 includes the entire range of instrumentation shown in **Fig. 1**C. This US transducer network allows combined passive and active US stress wave monitoring, which is introduced in [10]. In this research, it was employed to monitor (a) the development of UHPFRC properties at the early age within the formwork (Phase 1), (b) the response during load testing after 28 days (Phase 2), and (c) the response during environmental temperature variation (Phase 3).

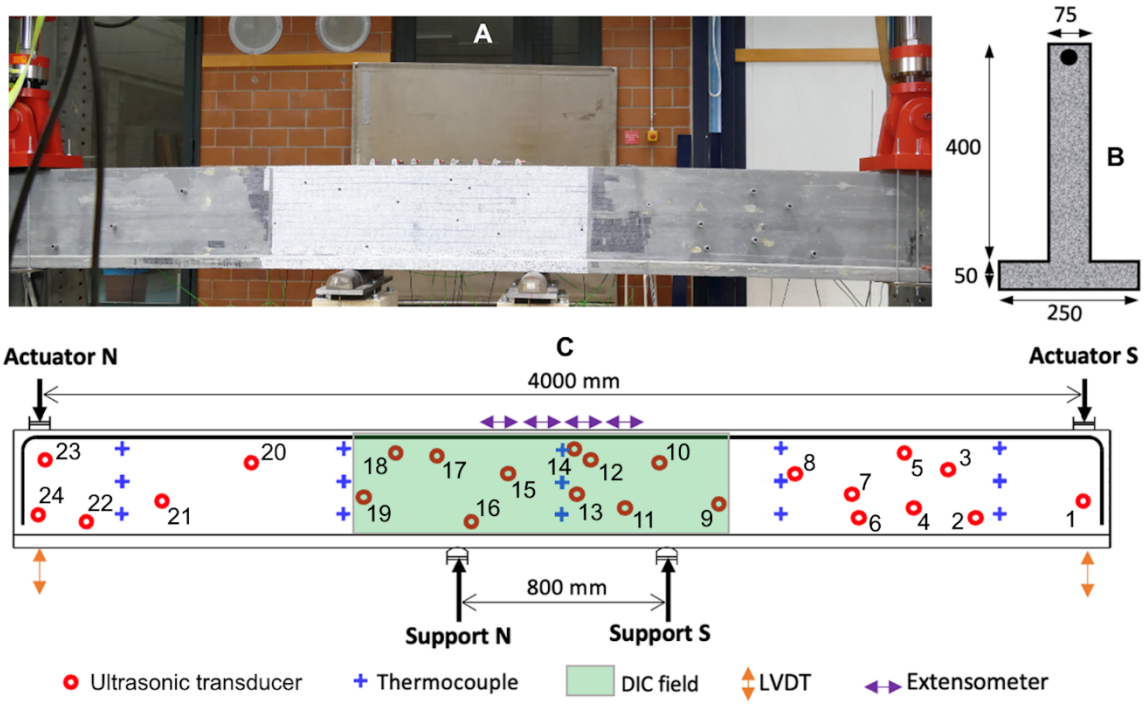

Fig. 1 A) Experimental test setup of Phase 2; B) Specimen cross-section; C) instrumentation: Phase 1: Only US transducers and thermocouples were used, Phase 2: Everything shown was used.

3. Early-age monitoring (Phase 1)

The first phase of the monitoring involved measuring the development of the early-age properties of UHPFRC, while the specimen was still in the formwork. Combined passive and active US stress wave monitoring started 2.7 hours after casting. A pulse is emitted by each US transducer sequentially every 30 minutes, and a recording is triggered using the other US transducers. The 24-transducer network produces a total of 552 emitter-receiver couples that can be used to analyse waveform properties such as amplitude, duration, and P-wave velocity. The evolution of the P-wave velocity of the US pulse is investigated in previous study [11,12]. The P-wave velocity significantly increased during the first 48 hours and then only slightly increased to approach a final value between 4200 and 5000 m/s given the US transducer couple (mean value of 4690 m/s with a standard deviation of 130 m/s). It has been demonstrated that the P-wave velocity measurements lead to an accurate evaluation of the evolution of the UHPFRC elastic modulus during early age. From this early-age monitoring, it can be concluded that this novel monitoring system can accurately monitor the evolution of the UHPFRC properties, but a large number of measurements (meaning a large number of US transducer couples) are needed as individual measurements may present large variability.

4. Load testing (Phase 2)

4.1. Loading protocol and monitoring procedure

In the second monitoring phase (Phase 2), the specimen was loaded following the loading protocol shown in **Fig. 3** using a four-point bending configuration. The loading protocol involved repeating three loading-unloading cycles at a given load level, referred to as load cycle group (LCG). Between LCG, one load cycle representative of in-service conditions was applied (26 kN). Peak loads for each LCG and for each actuator were 13, 26, 39, 52, 65, 78, 91, and 104 kN. During the last loading (labelled “F”), the load was increased

monotonically until the specimen failed at a load of 105 kN. The experiment was performed in displacement-controlled mode to ensure stable loading conditions.

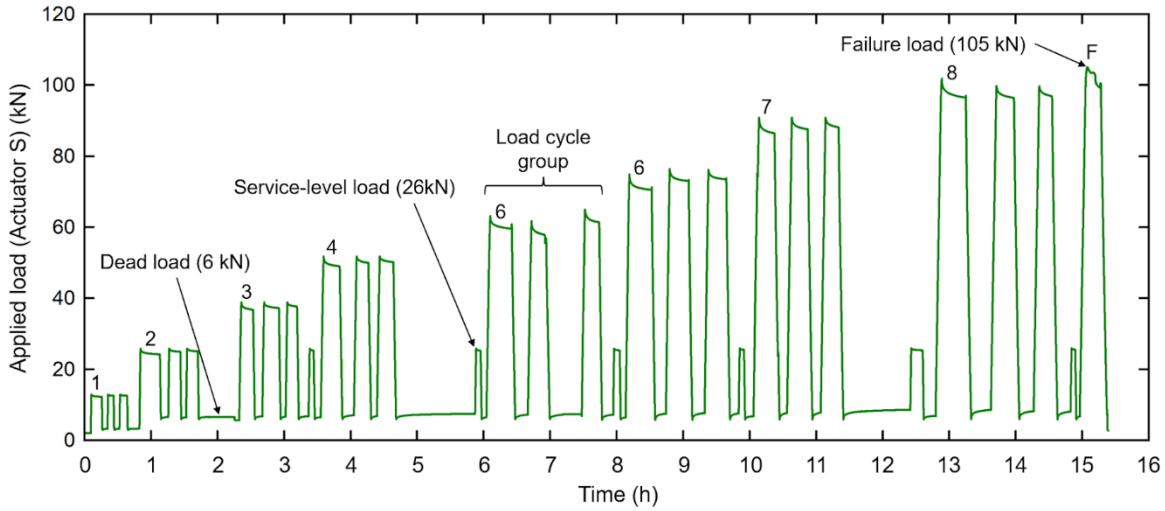

Fig. 2 Illustration of loading protocol: Load (Actuator S) vs. time. LCG are numbered with the number being located at the first loading cycle of that group.

An AMSY-6 AE data recorder from Vallen Systeme GmbH was used for both passive and active US stress wave monitoring and a sampling rate of 5 MHz was used to digitize transient US waveforms for a duration of 3.28 and 6.55 ms, respectively. Monitoring was divided by LCG to keep file sizes manageable. While passive US stress waves (or AE) were recorded throughout the test, active US stress wave monitoring was performed (a) during the service-level load being applied, (b) prior to each load cycle (with only the self weight being applied), (c) while the load of a LCG was being applied (after AE hit rates had notably subsided), and (d) after unloading was completed (with again only the dead load being applied). This process is illustrated in **Fig. 3** for LCG 4 (peak load = 52 kN) with passive and active US stress wave monitoring hit amplitudes being shown as light blue and red dots, respectively. The blue curve is a sample LVDT displacement shown for reference.

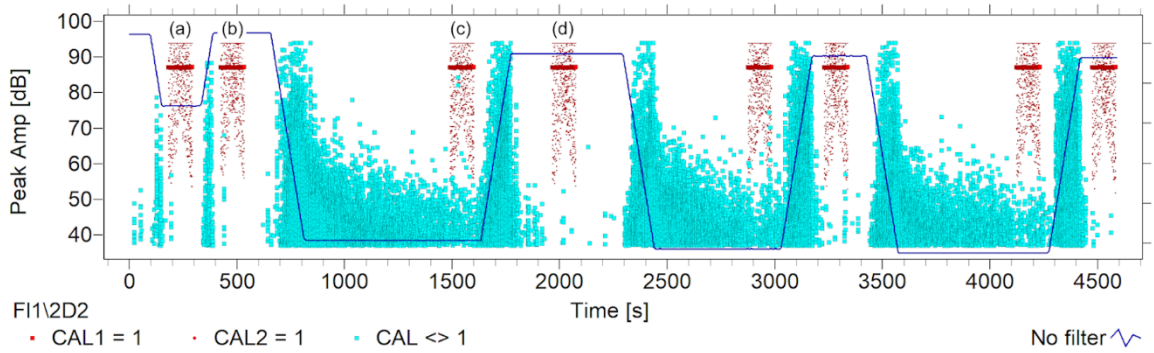

Fig. 3 Sample passive (light blue dots) and active (red dots) US waveform hit amplitudes (all US transduces) for LCG 4. The displacement history of a sample LVDT (blue curve) is shown for reference (arbitrary scaling).

4.2. Structural response of test specimen

During the final loading cycle "F", ductile failure of the beam occurred at a load of 105 kN (one actuator). The failure crack appeared in the bending-only region between the supports of the beam (**Fig.** 4). Note that a crack had already initiated early on, which can be seen by the strain field shown in **Fig. 4**B, Image I. After the beam displacement (deflection) reached a value of about 45 mm, the test was discontinued. A large crack [see **Fig. 4**B, Image IV)] and beam displacement remained after unloading. As can be observed from the load vs.

displacement curve (**Fig. 5**A), the specimen responded, by visual observation, only slightly non-linearly until LCG 8 was applied (peak load = 104 kN).

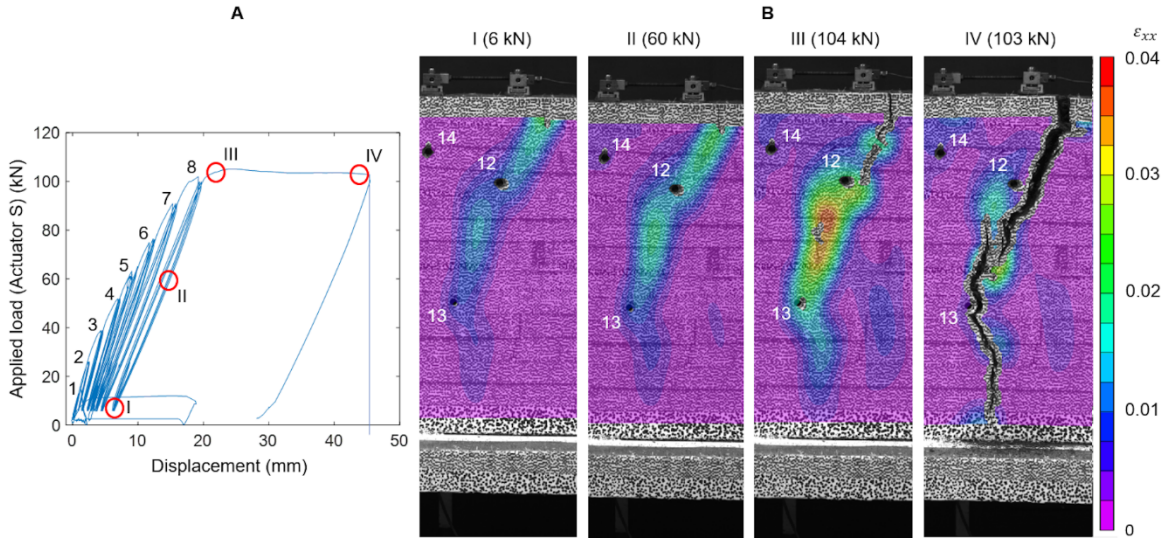

Fig. 4 Performance of UHPFRC beam specimen for Phase 2. A) load (Actuator S) vs. beam displacement for entire Phase 2. LCG are numbered 1 through 8; B) DIC-computed strain field results for final loading leading to failure.

4.3. Evolution of P-wave velocities

Using active US stress wave monitoring, P-wave velocities were calculated for all US transducer couples over the duration of Phase 2. Results for selected US transducer couples are presented in **Fig. 5**. Transducer couples involve US transducer 12, which is located near the failure crack (see **Fig. 4**B), and US transducer Couple 1-2, which is in the uncracked portion of the beam. P-wave velocity values were determined at the unloaded load level, after unloading [labeled (b) and (d) in in **Fig. 3**], and the results were normalized with the initial P-wave velocity.

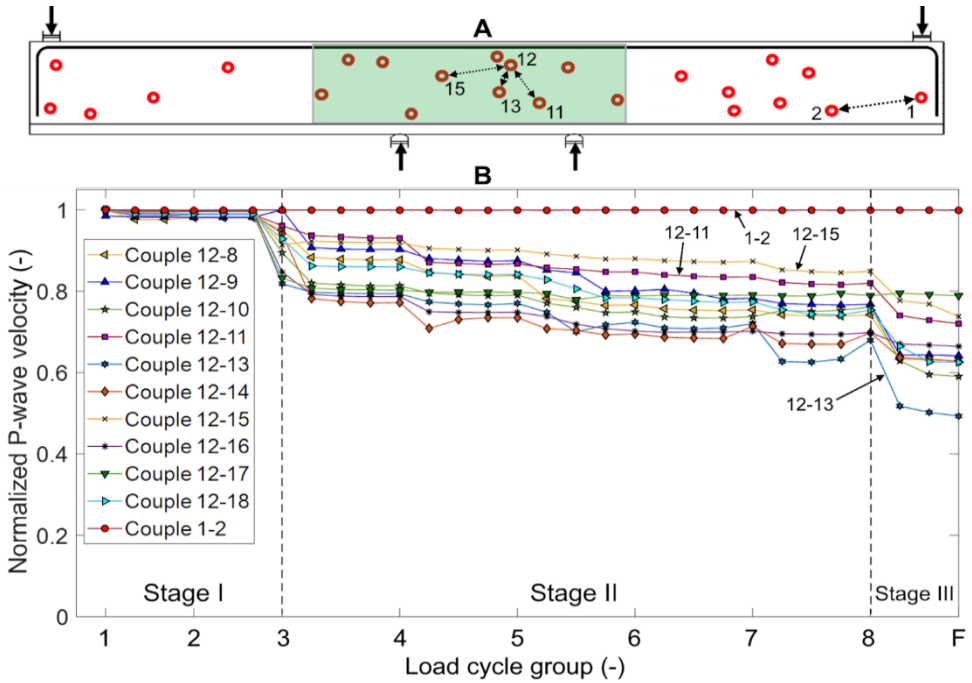

Fig. 5 Evolution of P-wave velocities vs. LCG for select US transducer couples. LCG are numbered with the number being located at the first loading cycle of that group.

A decreasing P-wave velocity means that cracking has occurred during the previous load cycle between two US transducers. Overall, a trend exists for P-wave velocities to decrease with an increasing number of load cycles. For all US transducer couples shown in **Fig. 5**, the P-wave velocity measurements remain relatively constant for LCG 1 and 2, meaning that the beam remains in the elastic domain (Stage I). After the first loading cycle of LCG 3 was applied, the P-wave velocities for all couples involving US transducer 12 decrease, initiating Stage II, which is when UHPFRC enters strain hardening. This degradation is observed for all US transducer couples in the maximum-bending area, showing a relatively uniformly distributed degradation. After LCG 8, a second important drop is observed, which corresponds to the first loading-unloading cycle at 104 kN (99% of the maximum load), meaning that additional damage occurred at this load level (Stage III). This result was confirmed by visual observations and conventional monitoring, where critical crack propagation was clearly visible. Defining the end of the elastic domain of a UHPFRC beam is challenging and requires complex inverse-analysis procedures [13]. The monitoring approach proposed in this study, which is highly sensitive to small changes of the material properties, clearly shows the end of the elastic domain (Stage I). The next subsection discusses the approach's ability to capture cracking by employing source localization.

4.4. Localization of US stress wave sources

Locating US stress wave sources was performed for both passive and active US stress wave sources. Traditionally done for passive US stress wave (or AE) sources [14], here, selected results for both monitoring approaches are presented and compared.

In this study, US stress wave sources are located using a traditional Geiger method-based source location algorithm. Locations were estimated in 2D, assuming this simplification is appropriate given the geometry of the beam specimen. The software VisualAE from Vallen Systeme GmbH [15] was used for this purpose, using the following settings:

- The P-wave velocity, $V_P = 4715$ m/s is based on the data discussed in Section 3.
- P-wave arrival time picking was performed using an AIC-based picker [14].
- A minimum of four and a maximum of six P-wave arrival times were used to create an event and compute a source location estimate. This was found to lead to the most accurate source location estimates.
- Location uncertainty (LUCY) was calculated as the square root of the mean of the squared differences between a set of computed and observed arrival time differences, each of which is multiplied by the assumed P-wave velocity. LUCY represents a measure of the goodness-of-fit of the source location estimation.
- A filter with LUCY ≤ 50 mm was set to ensure only the most accurate source location estimates are used for further analysis and interpretation.

Passive US stress wave monitoring captures the energy released during fracture processes within a material resulting from an external stimulus in real-time. In this laboratory study, primary sources such as micro- and macro-cracking due to mechanical loading are the expected causes. In a real-world setting, secondary sources and environmental noise are likely to occur and need to be considered [16].

Fig. 6 shows select source location results from passive US stress wave (or AE) monitoring. The presented results include source location estimates from the loading and holding portion of the first cycle of each LCG. Note that the area of the failure crack already shows a notable number of passive US stress wave sources during LCG 2, which is at a load of 26 kN. Also, the pattern closely matches the shape of the failure crack (see **Fig. 4**B). After LCG 3, the level of passive US stress wave sources decreases until load cycles LCG8 and 9 are reached, of which the latter corresponds to the failure load.

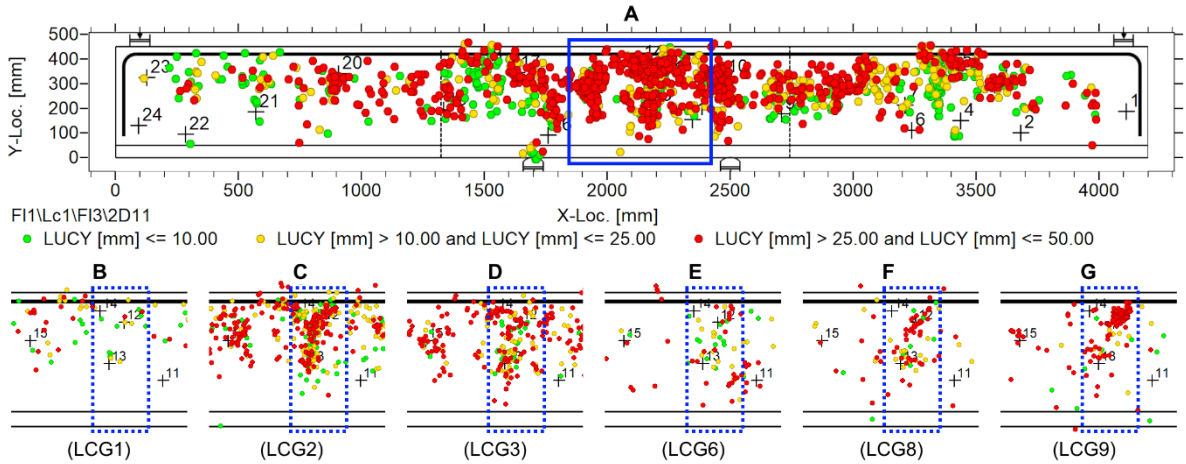

Fig. 6 Select passive US stress wave (or AE) source location estimates. A) Elevation view of UHPFRC test beam; B) through G) Beam areas corresponding to blue box shown in A for select LCG. The dashed blue boxes in A) through G) is the area corresponding to the strain field shown in **Fig. 4**B.

Fig. 7 shows summary statistics of select source location estimates from both passive and active US stress wave monitoring. **Fig. 7**A shows the LUCY corresponding to the results presented in **Fig. 6** for each LCG. It can be observed that there is a trend for the average LUCY to increase with increasing load cycles, which can be explained by the increasing level of cracking of the beam specimen, which interferes with the direct wave path of the US stress waves. Note that the standard deviations are almost the same for all LCG and are large enough to make it impossible to use LUCY as a reliable quantitative predictor. In **Fig. 7**B, source location results from active US stress wave monitoring are presented. Here, a similar trend exists for LUCY to increase with increasing load cycles. Note that significant increase in LUCY after LCG 2, which directly correlates to leaving the elastic domain. This further correlates to the notable passive US stress wave sources observed in **Fig. 6**C.

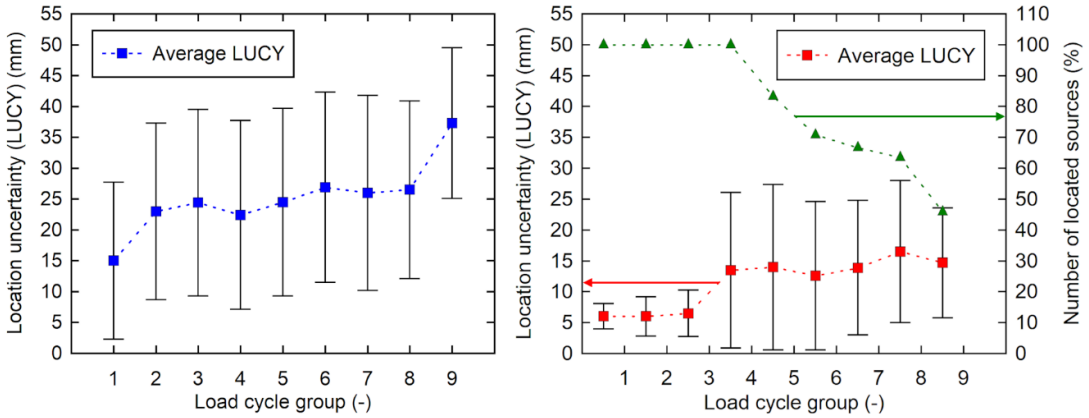

Fig. 7 Summary statistics of select source location estimates. A) Average location uncertainty (LUCY) vs. LCG for passive sources; B) Average LUCY and percentage of located sources vs. LCG for active sources. Error bars represent ± one standard deviation of the data.

5. Conclusions

This paper introduces a novel monitoring approach to measure UHPFRC properties continuously and accurately from an early age to the failure phase. The sensor network involves 24 US transducers that have been embedded in a 4.2-meter-long beam specimen. Continuous monitoring using combined passive US stress wave (or AE) and active US stress wave monitoring enables the accurate characterization of the evolution of UHPFRC properties, such as the elastic modulus during the very early age (Phase 1), as well as damage progression (end of elastic domain, crack location, propagation) of the beam during the load

testing phase (Phase 2). Notably, with the proposed monitoring approach it was possible to predict the location and shape of the failure crack of the UHPFRC laboratory beam at a level of approximately 25% of the observed failure load, which is in-service loading conditions. The presented monitoring approach offers new perspectives on developing holistic structural monitoring from an early age to structural failure or decommission, offering the potential for infrastructure owners to make informed asset management decisions based on quantitative data. Future work includes a detailed analysis of damage localization and quantification.

Acknowledgements

The experiment was conducted in the EPFL Structural Engineering Platform (GIS). Technical support for formwork and specimen fabrication as well as instrumentation was provided by Gilles Guignet (technical coordinator), François Perrin, Léa Frédérique Dubugnon, and Luca Mari.

References

[1] Habel K, Viviani M, Denarié E, Brühwiler E. Development of the mechanical properties of an Ultra-High Performance Fiber Reinforced Concrete (UHPFRC). Cement and Concrete Research 2006;36:1362–70.

[2] Toutlemonde F, ROENELLE P, Hajar Z, Simon A, LAPEYRERE R, Martin R, et al. Long-term material performance checked on world's oldest UHPFRC road bridges at Bourg-Lès-Valence, Marseille, France: 2013, p. 265–74.

[3] Brühwiler E, Denarié E. Rehabilitation and Strengthening of Concrete Structures Using Ultra-High Performance Fibre Reinforced Concrete. Structural Engineering International 2013;23:450–7.

[4] Graybeal B, Brühwiler E, Kim B-S, Toutlemonde F, Voo YL, Zaghi A. International Perspective on UHPC in Bridge Engineering. Journal of Bridge Engineering 2020;25:04020094.

[5] Bertola N, Schiltz P, Denarié E, Brühwiler E. A Review of the Use of UHPFRC in Bridge Rehabilitation and New Construction in Switzerland. Frontiers in Built Environment 2021;7:155. https://doi.org/10.3389/fbuil.2021.769686.

[6] Brühwiler E. UHPFRC technology to enhance the performance of existing concrete bridges. Structure and Infrastructure Engineering 2020;16:94–105. https://doi.org/10.1080/15732479.2019.1605395.

[7] Swiss Society of Engineers and Architects. Ultra-High Performance Fibre Reinforced Cementitious composite (UHPFRC) – Materials, dimensioning and execution 2024.

[8] Kamen A, Denarié E, Sadouki H, Brühwiler E. Thermo-mechanical response of UHPFRC at early age — Experimental study and numerical simulation. Cement and Concrete Research 2008;38:822–31.

[9] Niederleithinger E, Wolf J, Mielentz F, Wiggenhauser H, Pirskawetz S. Embedded Ultrasonic Transducers for Active and Passive Concrete Monitoring. Sensors 2015;15:9756–72.

[10] Schumacher T, Niederleithinger E. Combining Passive and Active Ultrasonic Stress Wave Monitoring Techniques: Opportunities for Condition Evaluation of Concrete Structures. NDT-CE 2022 - The International Symposium on Nondestructive Testing in Civil Engineering Zurich, Switzerland, August 16-18, 2022 2022.

[11] Bertola N, Schumacher T, Niederleithinger E, Brühwiler E. Combined Passive and Active Ultrasonic Stress Wave Monitoring of UHPFRC Properties on a Structural Level. vol. 3, Wilmington, Delaware, USA: Iowa State University Digital Press; 2023. https://doi.org/10.21838/uhpc.16652.

[12] Bertola N, Schumacher T, Niederleithinger E, Brühwiler E. Mesures de l'évolution des propriétés du CFUP en combinant les émissions acoustiques (passifs) et des ultrasons (actifs). Academic Journal of Civil Engineering 2023;41:150–8.

[13] Sawicki B, Brühwiler E, Bassil A. Deformational behavior and damage mechanism of R-UHPFRC beam subjected to fatigue loading. Mater Struct 2021;54:158. https://doi.org/10.1617/s11527-021-01745-3.

[14] Kurz JH, Schumacher T, Linzer L, Schechinger B, Grosse CU. Source Localization. In: Grosse CU, Ohtsu M, Aggelis DG, Shiotani T, editors. Acoustic Emission Testing: Basics for Research – Applications in Engineering, Cham: Springer International Publishing; 2022, p. 117–71. https://doi.org/10.1007/978-3-030-67936-1_6.

[15] Home - Vallen Systeme n.d. https://www.vallen.de/ (accessed April 20, 2024).

[16] Schumacher T, Schechinger B, Vogel T. AE Monitoring of Real Structures: Applications, Strengths, and Limitations. In: Grosse CU, Ohtsu M, Aggelis DG, Shiotani T, editors. Acoustic Emission Testing: Basics for Research – Applications in Engineering, Cham: Springer International Publishing; 2022, p. 731–52.